Protein Expression and Purification 175 (2020) 105697

Contents lists available at ScienceDirect

Protein Expression and Purification

journal homepage: www.elsevier.com/locate/yprep

Expression of a heptelidic acid-insensitive recombinant GAPDH from *Trichoderma virens*, and its biochemical and biophysical characterization

Shikha Pachauri[a,b], Gagan D. Gupta[b,c], Prasun K. Mukherjee[a,b,**], Vinay Kumar[b,*]

[a] Nuclear Agriculture and Biotechnology Division, Bhabha Atomic Research Centre, Trombay, Mumbai, 400085, India
[b] Homi Bhabha National Institute, Anushaktinagar, Mumbai, 400094, India
[c] Radiation Biology & Health Sciences Division, Bhabha Atomic Research Centre, Trombay, Mumbai, 400085, India

ARTICLE INFO

Keywords:
Trichoderma virens
GAPDH
Protein purification
Koningic acid
Secondary metabolism

ABSTRACT

Trichoderma virens genome harbors two isoforms of GAPDH, one (gGPD) involved in glycolysis and the other one (vGPD) in secondary metabolism. vGPD is expressed as part of the "vir" cluster responsible for the biosynthesis of volatile sesquiterpenes. The secondary metabolism-associated GAPDH is tolerant to the anti-cancer metabolite heptelidic acid (HA), produced by *T. virens*. Characterizing the HA-tolerant form of GAPDH, thus has implications in cancer therapy. In order to get insight into the mechanism of HA-tolerance of vGPD, we have purified recombinant form of this protein. The protein displays biochemical and biophysical characteristics analogous to the gGPD isoform. It exists as a tetramer with *T*m of about 56.5 °C, and displays phosphorylation enzyme activity with *K*m and *K*cat of 0.38 mM and 2.55 sec^{-1}, respectively. The protein weakly binds to the sequence upstream of the *vir4* gene that codes for the core enzyme (a terpene cyclase) of the "vir" cluster. The EMSA analysis indicates that vGPD may not act as a transcription factor driving the "vir" cluster, at least not by directly binding to the promoter region. We also succeeded in obtaining small crystals of this protein. We have constructed structural models of vGPD and gGPD of *T. virens*. *In silico* constrained docking analysis reveals weaker binding of heptelidic acid in vGPD, compared to gGPD protein.

1. Introduction

Glyceraldehyde 3-phosphate dehydrogenase (GAPDH, EC 1.2.1.12) is a glycolytic enzyme catalyzing the oxidative phosphorylation of glyceraldehyde 3-phosphate. GAPDH is also known to perform alternate non-metabolic functions, like DNA replication and repair, gene expression and signal transduction [1–3]. The multi-functionality of GAPDH is attributed to oligomerization, differential localization, complex formation with other proteins, and chemical modifications [2,4–6]. The functional diversity is also brought about by the presence of isoforms of GAPDH gene in some antibiotic-producing organisms. For instance, *Streptomyces arenae* produces pentalenolactone antibiotic, a sesquiterpene metabolite, that irreversibly inactivates GAPDH by binding at the active site [7]. *Streptomyces arenae* protects its own GAPDH from the antibiotic by the deployment of an alternate isoform of GAPDH (an additional copy present in the genome and associated with the pentalenolactone gene cluster) which is less sensitive to this metabolite [8].

Trichoderma virens produces heptelidic acid (HA), a selective inhibitor of GAPDH [9]. This is a sesquiterpene lactone which irreversibly inhibits GAPDH by binding to the sulfhydryl group of the active-site cysteine residue [10]. *T. virens* also possesses an isoform of GAPDH which is tolerant to heptelidic acid, and it takes over the glycolytic activity when heptelidic acid is being produced by *T. virens* [11]. The HA-tolerant GAPDH (named hereafter as vGPD) is encoded by a different gene and is not a modification of the glycolytic or heptelidic acid-sensitive GAPDH. The vGPD is associated with a secondary metabolism related gene cluster in *T. virens* and in a few *Aspergillus* spp. genomes [12,13]. This gene cluster, known as "vir" cluster, is responsible for the biosynthesis of volatile sesquiterpenes. In *Aspergillus oryzae*, this cluster has been reported to be responsible for the biosynthesis of HA [14]. They showed that deletion of *vGPD* gene does not affect the biosynthesis of HA. However, vGPD protein is tolerant to HA and performs glycolytic function when HA is produced by *A. oryzae*. Using gene knock-out approach, we had demonstrated that deletion of vGPD encoding gene in *T. virens* impairs biosynthesis of the same set of volatile sesquiterpenes reported earlier [15].

In the present study, we have expressed the HA-tolerant GAPDH

* Corresponding author.
** Corresponding author. Nuclear Agriculture and Biotechnology Division, Bhabha Atomic Research Centre, Trombay, Mumbai, 400085, India.
E-mail addresses: prasunmukherjee1@gmail.com (P.K. Mukherjee), vkbhatia@gmail.com (V. Kumar).

https://doi.org/10.1016/j.pep.2020.105697
Received 7 April 2020; Received in revised form 8 June 2020; Accepted 26 June 2020
Available online 16 July 2020

(vGPD) of *T. virens* in *E. coli* and studied its biochemical and biophysical characteristics as a first step to understand the differences between these two isoforms-one sensitive and the one tolerant to heptelidic acid, an anticancer compound targeting the Warburg effect.

2. Materials and methods

2.1. Bacterial strains

Escherichia coli strain DH5α (Novagen) was used for vector amplification. pNH-TrxT plasmid from Opher Gileadi (Addgene plasmid # 26,106) and *E. coli* BL21 star (DE3) strain (Novagen) were used as expression vector and host strain, respectively.

2.2. Reagents

The following chemicals and reagents were obtained from the indicated commercial sources: Luria Bertani (LB) broth and LB agar (HiMedia Laboratories, Mumbai); Isopropyl β-D-1-thiogalactopyranoside (IPTG), EDTA, phenylmethylsulfonyl fluoride (PMSF), SYPRO orange dye, Tris(2-carboxyethyl) phosphine hydrochloride (TCEP), β-nicotinamide adenine dinucleotide (NAD+), DL-glyceraldehyde 3-phosphate solution (all from Sigma Aldrich); Ni-IDA matrix (GE Healthcare), unstained protein molecular weight (MW) marker (Fermentas); restriction enzymes and *Taq* polymerase (New England Biolabs).

2.3. Cloning of gene for vGPD in E. coli

The gene for vGPD was PCR-amplified from the EST clone obtained from the cDNA library of *T. virens* [37]. The primer sequences for the amplification of the full-length *vGPD* cDNA (and other primers) are given in Supplementary Table S1. The PCR product was purified using PCR product purification kit (Sigma Aldrich) and ligation independent cloning method was utilized for cloning of PCR amplified *vGPD* gene into pNH-TrxT expression vector yielding pNH-TrxT-vGPD construct. The recombinant pNH-TrxT-vGPD construct was transformed into the cloning host, *E. coli* DH5α competent cells, and the transformed cells were grown onto LB agar plates (supplemented with 25 μg/ml of kanamycin) at 37 °C. Colony PCR using *Taq* DNA polymerase was performed for selection of transformed colonies and the recombinant plasmid was purified using a plasmid purification kit (Qiagen) and sequenced.

2.4. Expression and purification of vGPD protein

For vGPD protein expression, the purified pNH-TrxT-vGPD plasmid was transformed into the expression host BL21 Star (DE3). The transformed *E. coli* BL-21 cells harboring the recombinant plasmid construct pNH-TrxT-vGPD were cultured in 5 mL LB medium (containing 25 μg/ml of kanamycin) at 37 °C overnight. The primary culture was diluted (1:100) into fresh LB containing 25 μg/ml of kanamycin. The recombinant cells were grown at 37 °C in LB medium supplemented with 50 μg/ml of kanamycin until OD_{600} reached 0.6. Higher concentration of the antibiotic was used during large-scale protein expression to avoid bacterial contamination. Expression of protein was induced by adding 0.5 mM IPTG followed by shaking at 18 °C overnight. The cells expressing recombinant protein were harvested by centrifugation at 10,000 *xg* for 5 min and re-suspended in buffer A (20 mM Tris-HCl (pH 8.0), 300 mM NaCl, 20 mM imidazole, 10% glycerol, 1 mM PMSF, 2 mM NAD+, 2 mM TCEP and 0.2 mM EDTA) and containing 1 mg/ml lysozyme. The re-suspended cells were stored at −80 °C until further use. The cells were thawed at room temperature and then lysed using a sonicator on ice for 10 min at 30% duty cycle in pulse mode (3 s ON, 3 s OFF). The lysed cells were centrifuged at 21,000 *xg* for 30 min at 4 °C and the clear supernatant was collected in a fresh autoclaved centrifuge tubes for further purification steps. The recombinant vGPD protein was purified using Ni-iminodiacetic acid (Ni-IDA) matrix pre-equilibrated with buffer A containing 20 mM imidazole to avoid nonspecific binding of the protein. The clear supernatant of the cell-free extract containing recombinant vGPD protein with histidine-tag was loaded onto the pre-equilibrated column. The flow-through from the column was collected. The column was washed with 20 column volume of buffer A containing 50 mM imidazole to remove non-specifically bound proteins and the wash-through was also collected. The protein was eluted to near homogeneity using the same buffer containing 100 mM–300 mM imidazole. Eluted fractions were subjected to SDS-PAGE analysis and the fractions containing the recombinant protein were pooled. Overnight dialysis was performed in order to remove imidazole from the protein. The protein was concentrated using corning spin-X UF concentrators (10K MWCO, CLS431478 Sigma Aldrich) and stored in a storage buffer containing (20 mM Tris-HCl (pH 8.0), 100 mM NaCl, 10% glycerol, 1 mM PMSF, 2 mM NAD+ and 2 mM TCEP). The protein concentration was determined using modified Folin-Lowry's method using bovine serum albumin (BSA, Fermentas) as a standard.

The identity of purified His-tagged vGPD protein was confirmed by the Western blotting. The purified vGPD protein was separated on 12% SDS-PAGE and transferred to polyvinylidene fluoride (PVDF) membranes by electro-blotting. The non-fat-dried milk bovine blocking solution (Sigma Aldrich) was used at working concentration of 3%. Membranes were washed with phosphate buffer saline (PBS) and then incubated for 1 h at room temperature with a 1:10,000 dilution of mouse monoclonal anti-His-tag antibody (SAB2702218-Sigma Aldrich). Blots were again washed with PBS buffer and incubated with alkaline phosphatase-conjugated rabbit anti-mouse IgG antibody (1:50,000 dilution; A4312-Sigma Aldrich), and the membranes were developed with 5-bromo-4-chloro-3-indolyl phosphate (BCIP) and nitro-blue tetrazolium (NBT) substrate (B1911-Sigma Aldrich). The molecular mass of the stable vGPD was estimated from MALDI-TOF analysis.

2.5. Phosphorylation activity assay

The oxidative phosphorylation activity of vGPD was assayed using micro-plate reader at 25 °C by monitoring NADH absorbance at 340 nm. The reaction mixture of 100 μL contained 15 mM sodium pyrophosphate buffer (pH 8.9), 30 mM sodium arsenate, 10 mM DTT, 7.5 mM β-nicotinamide adenine dinucleotide and 2 mM DL-glyceraldehyde 3-phosphate solution. All experiments and assays were carried out in triplicate. Initial velocities of the enzymatic reaction were determined by varying concentration of the substrate DL-glyceraldehyde 3-phosphate (G3P; from 0.02 to 4 mM). Kinetic parameters (*Km* and *Kcat*) were determined by fitting initial velocities with the Michaelis–Menten equation and graph was plotted using Origin 8.0 software. Rabbit muscle GAPDH was also subjected to assay as a positive control.

2.6. Biophysical characterization of vGPD protein

To probe the fold status and thermal stability of vGPD, intrinsic fluorescence spectrum and thermo-flour shift assays were performed. Intrinsic fluorescence was determined on a JASCO spectrofluorometer (FP-8500) at 25 °C. The intrinsic fluorescence spectrum of the vGPD protein (20 μM) was measured at an excitation wavelength of 280 nm and emission in the wavelength range of 300–400 nm with 1 cm pathlength cuvette. Three independent spectral measurements were averaged for determining intrinsic fluorescence spectrum of the vGPD protein.

The thermo-flour shift assay was performed in a 96-well plate containing protein concentration of 2 μM along with freshly diluted SYPRO orange dye (1:1000, v/v) in 25 μL reaction mixture, in triplicates. Lysozyme was also monitored as an internal control. PCR plates were then sealed and placed into a BioRad CFX96™ real-time PCR system in FRET mode. Thermal scanning was performed from 20 °C to

95 °C, every 30 s, in 1 °C increments. Subsequent analysis of the fluorescence data was done using software provided with the CFX96™ real-time system. Three independent measurements were averaged for determining melting temperature for the tertiary structure of the vGPD protein.

2.7. Molecular weight determination

Superdex™ 200 GL column (Pharmacia) on AKTA purifier (GE Healthcare) was used for determining the molecular weight and oligomeric state of vGPD protein. The column was pre-calibrated with standard molecular weight markers (Chymotrypsinogen- 25 kDa, Ovalbumin- 44 kDa, Bovine serum albumin – 66.5 kDa, Aldolase – 158 kDa, Catalase- 250 kDa) and standard curve was plotted with elution volume *v/s* the logarithm of molecular weight of markers. Conformational integrity of vGPD and its molecular weight were also checked by electrophoresis on 10% non-denaturing polyacrylamide gel (Native-PAGE). Dynamic Light Scattering (DLS) was employed to characterize the hydrodynamics properties and DLS curve was analysed for determining homogeneity and polydispersity of the recombinant vGPD protein.

2.8. Protein crystallization

Initial crystallization attempts were made using oil drop method in 96-well plate at 295 K using commercially available JCSG+ kit (Qiagen) and crystallization cryo kit (Sigma Aldrich). Hanging-drop and sitting-drop methods were used for performing crystallization with each drop of 2.5 μL protein (10 mg/ml) and 2.5 μL buffer.

2.9. Molecular modeling

Structural models of gGPD and vGPD proteins were constructed by I-TASSER server (http://zhanglab.ccmb.med.umich.edu/I-TASSER/ [16]). Both gGPD (64.2%) and vGPD (62.8%) proteins share high sequence identity with human GAPDH (PDB ID, 3h9eB [17]), which was identified as the top-hit by I-TASSER protocol. The protein models were validated using Ramachandran plot (http://mordred.bioc.cam.ac.uk/~rapper/rampage.php) for the stereochemical nature of the protein for favored and unfavored regions, and the loops in unfavored region of the protein were further refined using ModLoop server (https://modbase.compbio.ucsf.edu/modloop/[18]). The refined model structures with the best acceptable range of Ramachandran plot were validated by Verify3D (https://servicesn.mbi.ucla.edu/Verify3D/[19]) and visualized by PyMOL visualization tool.

2.10. Docking of heptelidic acid

Heptelidic acid forms covalent bond with active-site Cys-150 of GAPDH [20]. The atomic coordinates of heptelidic acid, an irreversible inhibitor of GAPDH, were obtained from PubChem compound database (https://www.ncbi.nlm.nih.gov/pccompound/) and the modelled structures of gGPD and vGPD proteins (this work) were used for molecular docking studies. The gGPD and vGPD protein structures and ligand structure (heptelidic acid) were pre-processed using Protein preparation wizard and a Ligprep module in Schrodinger suite 2019-4 (https://www.schrodinger.com/covdock [21]). Both the protein and the ligand structures were minimized using the OPLS3 force field. The CovDock protocol was used to perform covalent docking between heptelidic acid and active-site of proteins. Covalent docking was carried out by specifying Cys-150 (or its equivalent) at the active site of the proteins as reactive residue and the epoxide opening reaction was simulated for covalent bond formation. Covalently docked complexes were created using Glide module in Schrodinger suite 2019-4.

2.11. DNA binding activity of recombinant vGPD

Electrophoretic mobility shift assay (EMSA) was performed for analyzing interaction between vGPD protein and putative promoter region of *vir4* gene. The upstream region of *vir4* gene (~1600 bp) was used as the target DNA (double stranded; henceforth named as Pvir4) and ORF region of another gene of ~1700 bp (Trividraft_217322) was used as the non-specific DNA that was used for comparing the specificity of the vGPD protein for Pvir4 dsDNA. Both Pvir4 dsDNA and non-specific dsDNA were PCR amplified using sequence-specifc primers (Supplementary Table S1) and gel extracted. Approximately, 1 pmol concentrations of the purified Pvir4 dsDNA was labelled using 1 μCi [γ-^{32}P] ATP by T4 polynucleotide kinase. Different concentrations of purified recombinant vGPD proteins were added in 10 μL reaction mixture containing 20 fmol of labelled dsDNA in buffer B (50 mM Tris–HCl (pH 8.0), 75 mM KCl, 5 mM $MgSO_4$ and 0.5 mM DTT). For determination of specificity of vGPD protein for Pvir4 dsDNA, different concentrations of cold non-specific dsDNA were added in the reaction mixture containing saturating concentration of vGPD protein incubated with the labelled Pvir4 dsDNA. All the reactions were incubated at 37 °C for 20 min and loaded on 6% native-PAGE gels for separation of the bound and unbound fractions. Gels were dried using a vacuum gel dryer and were exposed to X-ray films overnight. Autoradiograms were developed and documented for image analysis. ImageJ 2.0 software was used for calculation of band intensity of bound and unbound fractions from each autoradiogram. The % bound fraction of Pvir4 dsDNA against increasing concentration of recombinant vGPD protein was plotted using GraphPad Prism 7. Theoretical fit of one-site specific binding kinetics model in GraphPad Prism 7 was used to calculate dissociation constant (*Kd*).

3. Results

3.1. Cloning, heterologous expression and purification of the T. virens vGPD protein

Several attempts were employed for the expression and purification of the vGPD protein but either the protein was not expressed or it expressed as insoluble aggregate. The susceptibility of the free thiol group at the active site of the protein could account for the instability of the protein followed by aggregation [22]. Thus, we employed pNH-TrxT vector which has a thioredoxin tag (~12 kDa) that helps in maintaining reduced environment in the bacterial cytoplasm and provides stability to redox sensitive-proteins. Full length vGPD was cloned into pNH-TrxT plasmid via ligation-independent cloning and then transformed into *E. coli* BL-21 expression host for protein expression and purification. The best condition for the recombinant protein expression was found to be induction with 0.5 mM IPTG for 16 h at 18 °C. The recombinant protein with N-terminal poly-His tag was purified to near homogeneity by immobilized metal affinity chromatography (IMAC). All the steps were performed at 4 °C in the presence of 1 mM TCEP, a reducing agent, to maintain reduced environment. Western blot analysis with anti-His antibody confirmed the purification of recombinant protein containing both poly-His tag and thioredoxin tag (Fig. 1). MALDI-TOF analysis of purified vGPD showed the mass of the protein to be 50.2 kDa corresponding to the estimated mass of 50 kDa of the recombinant construct with poly-His tag (~1.8 kDa) and thioredoxin tag (12 kDa).

3.2. vGPD protein exists as tetramer in solution

Purified vGPD protein was analysed on a Superdex™ 200 GL column. The protein eluted as a single peak, coinciding with the UV absorbance peak at a molecular weight of 200 kDa. Rabbit muscle GAPDH was also analysed on the same column and it eluted at the same elution volume (Fig. 2A). The vGPD protein was electrophoresed on 10% native-PAGE which showed that the protein migrated as a single

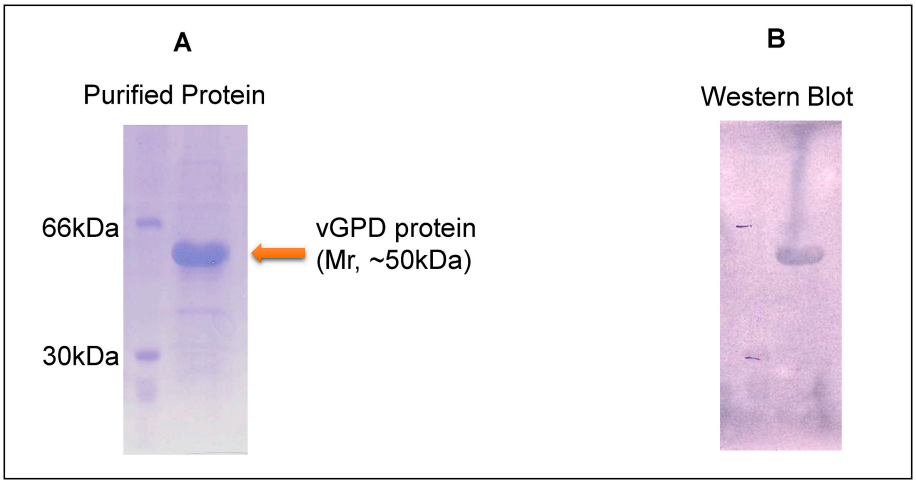

Fig. 1. Purification of vGPD by immobilized metal affinity chromatography, and Western blot with anti-His antibody. A) 15% SDS-PAGE gel showing recombinant vGPD protein (~50 kDa) purified using IMAC. **B)** Western blot analysis of the vGPD protein using anti-His antibody.

band parallel to 200 kDa protein band (Fig. 2B). The DLS profile with a narrow particle size distribution curve confirmed the homogeneity of the vGPD protein indicating monodisperse nature of the oligomer. The hydrodynamic diameter was estimated to be about 12.4 ± 2.5 nm (Fig. 2C). The polydispersity percentage of recombinant vGPD protein was estimated to be 17.3. Taken together, with the subunit mass of 50.2 kDa, as observed in MALDI-TOF analysis, it can be inferred that vGPD exists as a stable homo-tetramer (oligomer) in solution, like Rabbit muscle GAPDH. Tetramer as a biological significant oligomerization state has also been reported for 197 of the available 316 GAPDH entries in the Protein Data Bank (PDB).

3.3. Biophysical characterization of vGPD

Thermal denaturation of vGPD was scanned from 20 °C to 95 °C. The melting temperature for the tertiary structure (*T*m) of vGPD was determined to be 56.5 °C (Fig. 3A and B), which is in accordance with the secondary structure denaturation melting temperature of other GAPDH proteins from different organisms [23]. The *T*m of 69.5 °C for lysozyme, which was used as an internal control in this experiment, matched with the reported literature value. Intrinsic fluorescence spectrum analysis yielded information on the folded state of the vGPD protein. The spectrum result of vGPD protein shows an emission at 330 nm which is characteristic of buried tryptophan residues (Fig. 3C). Fluorescence spectrum of the 8 M urea treated denatured protein was found to show emission at 352 nm due to quenching of the fluorescence intensity by exposed tryptophan residues in the denatured protein (data not shown). The thermal denaturation and fluorescence studies thus confirm that recombinant vGPD protein adopts a globular fold similar to that of other known GAPDH proteins.

3.4. Kinetic analysis of the purified vGPD protein

Values of the Michaelis-Menten parameters, were calculated for the oxidation of G3P by recombinant vGPD protein. Michaelis-Menten plot was used for determining apparent values of *K*m, *V*max and *K*cat for vGPD protein; they were 0.38 mM, 3.19 μmol/min/mg and 2.55 sec^{-1}, respectively (Fig. 4). The *K*m for rabbit muscle GAPDH was determined to be 0.26 mM. Previous study reported *K*m values of 0.54 mM and 0.33 mM for vGPD and gGPD proteins [11].

3.5. Crystallization of vGPD protein

Crystals of vGPD were obtained using oil-drop method under two promising conditions containing- [Tris Na-citrate (0.1 M, pH 5.5), and PEG 2000 (20%)] and [calcium acetate (0.16 M), Na-cocadylate (0.08 M, pH 6.5), PEG 8000 (15%) and glycerol (20%)] as precipitants. Hanging-drop and Sitting-drop methods were also employed for

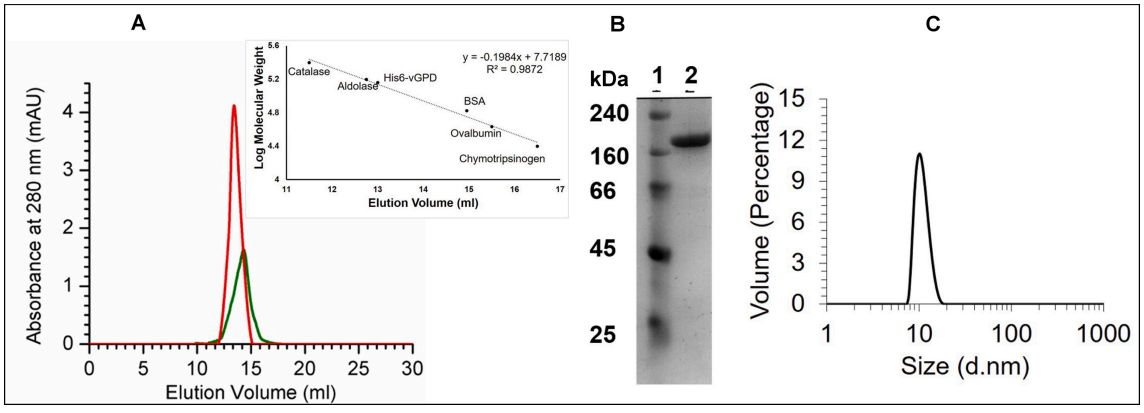

Fig. 2. Determination of molecular weight and oligomeric status of the purified recombinant vGPD protein. A) Elution profiles of vGPD (red colour) and rabbit muscle GAPDH (green colour) on Superdex™ 200 GL column. Molecular weight marker proteins (inset) used as standard were: chymotrypsinogen (25 kDa), BSA (66 kDa), ovalbumin (45 kDa), aldolase (160 kDa) and catalase (240 kDa). **B)** 10% native-PAGE. Lane 1, protein markers for native-PAGE; Lane 2, purified vGPD protein. **C)** Dynamic light scattering (DLS) analysis of recombinant vGPD protein showed a single sharp peak with hydrodynamic diameter of 12.4 ± 2.5 nm. The protein in solution behaved as mono-dispersive (estimated poly-dispersity ~ 17.3%).

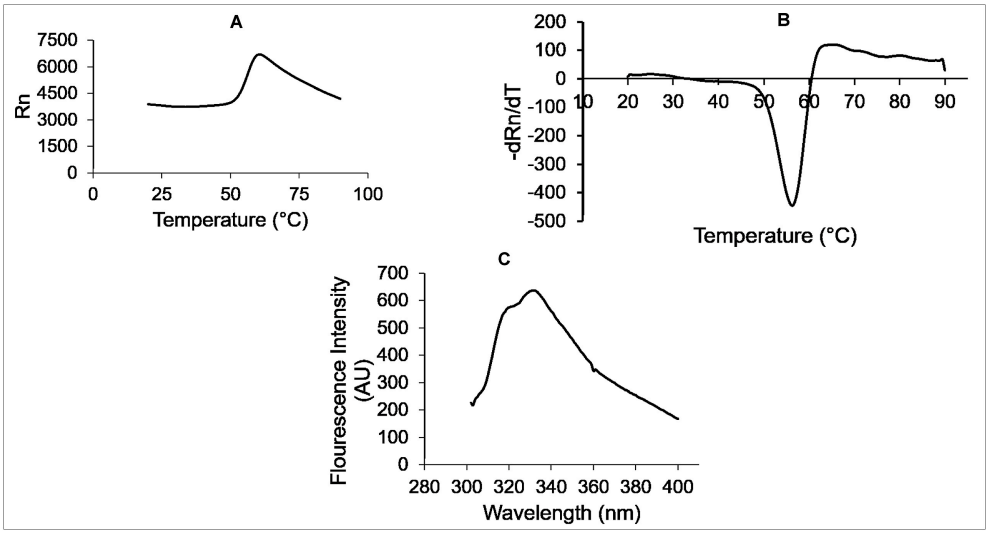

Fig. 3. Biophysical characterization of recombinant vGPD protein. A) Thermofluor-shift melt curve **B)** Derivative plot of thermofluor-shift melt curve **C) Intrinsic Trp fluorescence spectrum**. The vGPD protein (0.3 mg/ml) was dissolved in 25 mM Tris-HCl buffer (pH 7.6) and excitation wavelength was 280 nm. Intrinsic Trp fluorescence spectra were obtained by subtracting the spectra of the buffer. Three independent measurements were performed during thermofluor-shift and intrinsic fluorescence assays.

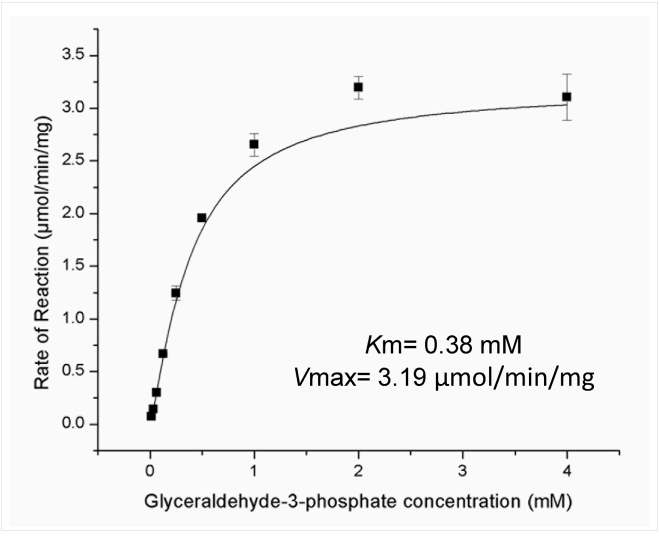

Fig. 4. Kinetics of vGPD enzyme activity. Initial velocity curve was fitted to the Michaelis-Menten equation using Origin lab 8.0 and the plot was used to determine *K*m and *V*max of vGPD protein. The reactions were monitored by estimating NADH production with increasing concentration of substrate (0.01 mM–4 mM) at 25 °C. Apparent *K*m, *V*max and *K*cat values for DL-glyceraldehyde 3-phosphate were calculated as 0.38 mM, 3.19 µmol/min/mg and 2.55 sec^{-1}, respectively.

crystallization under the similar conditions. However, very small crystals of dimensions about 5 µm were obtained which were not suitable for diffraction experiments (Fig. 5). Further optimization of buffer and PEG concentration was also performed to grow crystals of size suitable for single crystal diffraction analysis.

3.6. Molecular modeling of gGPD and vGPD proteins, and docking of HA

The gGPD and vGPD protein model structures were derived using GAPDH structure of *Homo sapiens* (PDB ID:3h9eB) as a template on the I-TASSER server. The models were validated and refined to best-fit by the on-line RAMPAGE (Ramachandran plot examination) tool. Ramachandran plot for gGPD model displayed that 94.9% residues are in the most favored region, 4.5% in the additional allowed region and only 0.6% residues in the outlier region. Similarly, 95.2% residues in the most favored region, 3.9% in the additional allowed region and only 0.9% residues in the outlier region of the Ramachandran plot were observed for the model for vGPD protein. The model structures for gGPD and vGPD were also assessed using Verify3D. The Verfiy3D analysis showed that 96.45% residues of the gGPD model and 98.81% residues of the vGPD structure have averaged 3D-1D score ≥0.2. These parameters showed good quality of vGPD and gGPD model structures.

The structure alignment of the selected models with each other and with the template individually by PyMol revealed that both the protein structures are highly conserved. The secondary-structure comparison with ESPript further revealed that gGPD and vGPD protein sequences from *Aspergillus* and *Trichoderma* share more than 80% similarity (~73% identity) with essentially conserved NAD+ cofactor- and substrate-binding sites (Supplementary Fig. S1). Notably, the two proteins

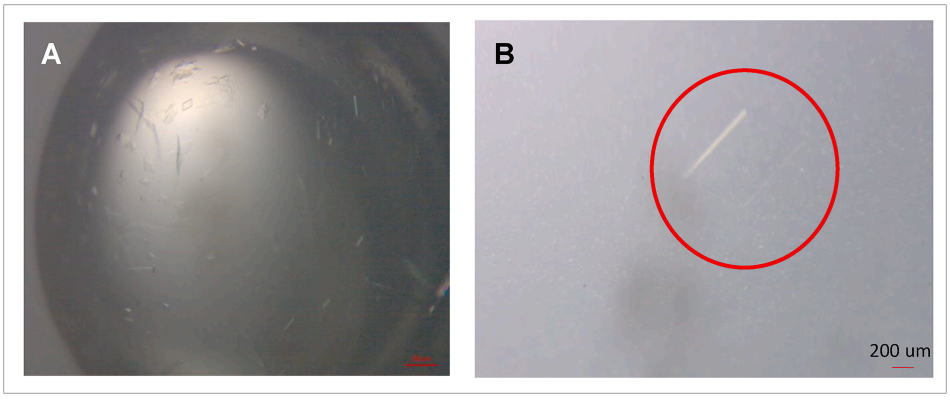

Fig. 5. Crystallization of vGPD protein. Protein was crystallized using sitting-drop vapor-diffusion method and commercial screens. Initial small crystals (**A**) obtained were further optimized (**B**) using optimized condition containing calcium Acetate (0.16 M), Na-cocadylate (0.08 M, pH 6.5), PEG 8000 (15%) and glycerol (20%).

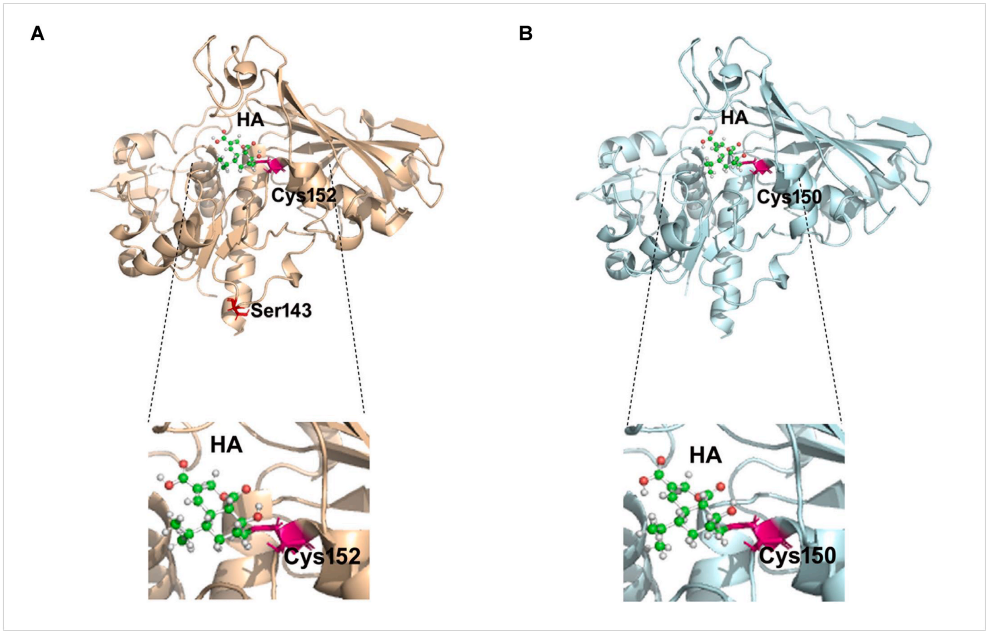

Fig. 6. Molecular modeling of the two isoforms of GPD (gGPD and vGPD) and docking of heptelidic acid ligand. A) gGPD-HA covalent docked structure. Residues Cys-152 and Ser-143 are labelled. **B**) vGPD-HA covalent docked structure with labelled Cys-150. Heptelidic acid (HA) is shown in ball-and-stick representation. The active site Cysteine residue and Serine residue are shown in red colour.

differ due to the presence of an INDEL in the loop-region placed at the entrance to active-site (Supplementary Fig. S1) [15]. This deletion-site (Ser-143 in gGPD) precedes the active-site scaffold of the GAPDH proteins and is situated on the surface loop in gGPD. The conserved indel could possibly introduce a number of modifications in the vGPD protein, like interaction with other proteins, change in subcellular location and post-translational modifications, and might add to the functional diversity of the protein [3].

We performed covalent docking using CovDock (https://www.schrodinger.com/covdock) and constraint that the irreversible inhibitor, heptelidic acid, formed covalent bond with the active-site cysteine residue, Cys-150 and Cys-152 of vGPD and gGPD proteins, respectively. This covalent binding mode of heptelidic acid in gGPD protein at the active site showed no interaction with the serine residue which is deleted in the vGPD protein. MM-GBSA binding energies were determined for both the covalently docked structures and heptelidic acid showed marginally higher affinity for gGPD protein as compared to vGPD protein with binding energy values of −49.63 and −43.67, respectively (Fig. 6). It is also likely, however, that deletion of Ser-143 in vGPD isoform alters conformation of the surface loop and restricts approach of HA to the active site.

3.7. vGPD protein binds non-specifically to the upstream region of vir4 gene

GAPDH has been addressed as a nucleic acid binding protein in several studies. Earlier knock-out studies also indicated differential effect on genes of the 'vir' cluster, suggesting that vGPD may be involved in the biosynthesis of volatile sesquiterpenes in *T. virens* [15]. The recombinant vGPD protein was purified to homogeneity from *E. coli* strain for performing electrophoretic mobility shift assay (EMSA) with [γ-^{32}P] ATP labelled Pvir4 dsDNA (~20 fmol). Binding assay with *vir4* gene was performed as it codes for the putative terpene cyclase, which is a core enzyme in the 'vir' cluster, and its deletion also abolished volatile sesquiterpene compounds production like vGPD deletion mutant. Specificity of vGPD protein for the radiolabeled Pvir4 dsDNA was examined by adding increasing amount (1–12 M excess) of cold non-specific dsDNA (NS-DNA) to the pre-incubated reaction mixture containing saturating concentration of the vGPD protein and radiolabeled Pvir4 dsDNA. This competition assay estimated that vGPD protein and Pvir4 dsDNA binding is non-specific with the equilibrium dissociation constant (*K*d) of 3.4 ± 0.21 μM (Fig. 7).

4. Discussion

GAPDH is classically known as a housekeeping protein catalyzing the sixth step in glycolysis. However, recent research suggests that the same protein has many auxiliary functions, like DNA replication and repair, gene expression and signal transduction [1–3]. An additional copy of GAPDH was earlier found in *T. virens* [11]. This GAPDH, which is tolerant to heptelidic acid, was proposed to takeover glycolysis function when this metabolite is produced by *Trichoderma* [11]. Maurer et al. [9] found a copy of GAPDH to be associated with a secondary metabolism-related gene cluster responsible for the biosynthesis of pentalenolactone in *Streptomyces arenae*. Mukherjee et al. [13] documented the association of additional copies of GAPDH with secondary metabolism-related gene clusters in *T. virens* and *Aspergillus* spp. We have recently demonstrated that this second GAPDH (vGPD), associated with the "vir" cluster, is involved in the biosynthesis of several volatile sesquiterpenes [15]. This GAPDH is thus an important subject of study because of two reasons: 1. How and why this GAPDH (vGPD) is involved in secondary metabolism and 2. What makes it tolerant to heptelidic acid that irreversibly inhibits the glycolytic GAPDH. One of the hallmarks of cancer cells is metabolic reprogramming. Due to Warburg effect, cancer cells have metabolic phenotypes like increased glycolysis [25]. GAPDH proved to be a preferred candidate for targeting glucose metabolism because it performs the important rate limiting step of glycolysis and produces first essential redox molecule i.e., NADH [26]. Secondly, metabolomics demonstrated that aerobic glycolysis in cancer cells flux through GAPDH and thus is an important regulatory enzyme in promoting Warburg effect [27]. Lastly, being moonlighting protein, GAPDH is also associated with many cancer progressing pathways like, protection against caspase-independent cell death, and increased proliferative index and cell cycle progression [25,28]. Anti-GAPDH therapeutic approach with natural inhibitor, heptelidic acid also known as koningic acid, for promoting anticancer effect has been recently demonstrated [24,29]. Even though the presence of HA-insensitive GAPDH in some fungal genomes has been known for decades, its mechanism is not known yet. The objective of the present study was to study in detail the HA-tolerant GAPDH at the protein level. However, several attempts (including different hosts, different vector, expression in yeast and expression in native host) did not yield significant amount of protein in soluble form. This is interesting, as several authors have earlier reported purification and crystallization of the glycolytic

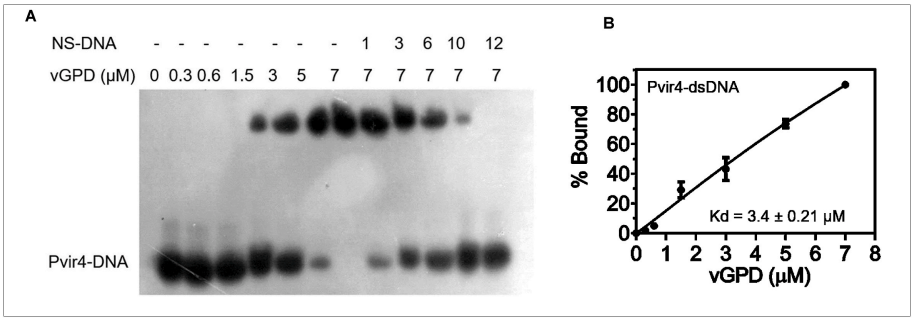

Fig. 7. Interaction of vGPD protein with the promoter region of *Vir4* gene (Pvir4). A) DNA-binding activity of vGPD protein with the upstream region of *vir4* gene in *Trichoderma virens* was determined using EMSA. PCR-amplified and gel purified Pvir4 DNA (20 fmol; ~1.6 kbp) was labelled with [γ-^{32}P] ATP and mixed with varying concentration to vGPD (0–7 μM). The mixtures were resolved on 6% native-PAGE. The competition assay performed by adding increasing amount of (1–12 M excess) cold non-specific DNA to the pre-incubated reaction mixture containing saturating concentration of the vGPD protein and radiolabeled Pvir4-DNA, suggests non-specific DNA-binding of vGPD. **B**) Measurement of the equilibrium dissociation constant (*K*d) by gel mobility shift assay.

GAPDH from many organisms [30–33]. We succeeded in getting the protein in soluble form by using the pNH-TrxT vector in *E. coli* expression system. The obtained value for *K*m of G3P for vGPD protein was similar to the *K*m value reported by Sakai et al. [11] for the HA-tolerant GAPDH purified from *T. virens*. The structural integrity of the recombinant vGPD protein has been confirmed by the thermo-flour shift assay that showed the apparent melting temperature of vGPD protein to be 56.5 ˚C and from the intrinsic fluorescence analysis which showed emission at 330 nm that is typical of partially buried tryptophan residues. Further, the recombinant protein displayed a single sharp peak in DLS analysis and oligomeric status of a homo-tetramer similar to other characterized GAPDH enzymes.

GAPDH has been widely addressed as a nucleic acid binding protein which is one of the moonlighting functions performed by it. The first study on GAPDH interaction with single stranded DNA was reported in 1977 by Perucho and colleagues [34]. Subsequently, many reports were published demonstrating DNA-mediated functions of GAPDH in regulation of mRNAs translation, binding with viral RNAs, nuclear tRNAs transport, telomere protection, gene regulation etc. Moreover, GAPDH is also associated with functions like apoptosis, DNA integrity maintenance and DNA repair mechanism which demands nuclear translocation. Nuclear functions of GAPDH are due to its oligomeric status, PTMs, oxidative stress and status of active-site –SH groups. However, in the present study we observed that vGPD protein can have non-specific interaction with the upstream region of putative *vir4* ORF (Pvir4 dsDNA) of approximately 1.6 kbp in *T. virens*. This study suggests that vGPD protein is not associated with the transcriptional regulation of "vir" cluster as *K*d is high. However, binding to this region mediated by other proteins cannot be ruled out. It is known that different proteins, like Siah1 and androgen receptor, are involved in forming complex with GAPDH and translocation of it inside the nucleus [35,36].

In silico analysis sheds some light on the possible subunit structure and differential affinity of the two GAPDHs towards HA. Both the *T. virens* proteins are expected to have similar tertiary structure and active-site scaffold, though from the partial amino acid sequences different molecular structures were advocated previously [11]. A notable difference in the two models is the location of conserved indel (residue Ser-143 of gGPD deleted in vGPD orthologs) [15]. This site is located in the surface loop that could alter interaction of the two isoforms with other proteins. It has earlier been demonstrated that isoform-I of GAPDH in *T. virens* (misidentified as *T. koningii*) is inhibited to the extent of 50% by 1 mM heptelidic acid but it is not affected at 0.1 mM of HA, while 50% inhibition was observed for isoform-II at 0.01 mM [11]. The covalent-docking of HA with the gGPD protein showed higher affinity in comparison to the vGPD protein (binding energy values of −49.63 vs −43.67 kcal/mol, respectively). The lower affinity towards vGPD compared to gGPD may be responsible for the observed inhibition data and also indicates that vGPD is responsible for the glycolysis in *Trichoderma* when heptelidic acid is produced, as suggested earlier [11].

Author contributions

SP performed laboratory experiments. GDG supervised protein purification. VK and PM conceptualised, designed and coordinated the studies. SP, VK and PM wrote the manuscript.

Author agreement statement

We the undersigned declare that this manuscript is original, has not been published before and is not currently being considered for publication elsewhere. We confirm that the manuscript has been read and approved by all named authors and that there are no other persons who satisfied the criteria for authorship but are not listed. We further confirm that the order of authors listed in the manuscript has been approved by all of us. We understand that the Corresponding Author is the sole contact for the Editorial process. He is responsible for communicating with the other authors about progress, submissions of revisions and final approval of proofs.

Declaration of competing interest

The authors declare no conflict of interest.

Acknowledgments

PKM thanks Dr. P. Suprasanna, Head, NA&BT Division, BARC, for encouragement and support. SP was supported by a fellowship from the Department of Atomic Energy, Government of India. SP would like to thank Dr. Ganesh Kumar Maurya for helping in EMSA experiment and analysis.

Appendix A. Supplementary data

Supplementary data to this article can be found online at https://doi.org/10.1016/j.pep.2020.105697.

References

[1] M.A. Sirover, New insights into an old protein: the functional diversity of mammalian glyceraldehyde-3-phosphate dehydrogenase, Biochim. Biophys. Acta Protein Struct. Mol. Enzymol. 1432 (2) (1999) 159–184.
[2] M.A. Sirover, On the functional diversity of glyceraldehyde-3-phosphate dehydrogenase: biochemical mechanisms and regulatory control, Biochim. Biophys. Acta Gen. Subj. 1810 (8) (2011) 741–751.
[3] C. Tristan, N. Shahani, T.W. Sedlak, A. Sawa, The diverse functions of GAPDH: views from different subcellular compartments, Cell. Signal. 23 (2) (2011) 317–323.
[4] M.A. Sirover, New nuclear functions of the glycolytic protein, glyceraldehyde-3-phosphate dehydrogenase, in mammalian cells, J. Cell. Biochem. 95 (1) (2005) 45–52.
[5] M. Zaffagnini, S. Fermani, A. Costa, S.D. Lemaire, P. Trost, Plant cytoplasmic GAPDH: redox post-translational modifications and moonlighting properties, Front. Plant Sci. 4 (2013) 450.
[6] A.A. Kosova, S.N. Khodyreva, O.I. Lavrik, Role of glyceraldehyde-3-phosphate

dehydrogenase (GAPDH) in DNA repair, Biochemistry (Mosc.) 82 (6) (2017) 643–654.
[7] S. Hartmann, J. Neeff, U. Heer, D. Mecke, Arenaemycin (pentalenolactone): a specific inhibitor of glycolysis, FEBS Lett. 93 (2) (1978) 339–342.
[8] K.H. Maurer, F. Pfeiffer, H. Zehender, D. Mecke, Characterization of two glyceraldehyde-3-phosphate dehydrogenase isoenzymes from the pentalenolactone producer *Streptomyces arenae*, J. Bacteriol. 153 (2) (1983) 930–936.
[9] A. Endo, K. Hasum, K. Hasumi, K. Sakai, T. Kanbe, Specific inhibition of glyceraldehyde-3-phosphate dehydrogenase by koningic acid (heptelidic acid), J. Antibiot. 38 (7) (1985) 920–925.
[10] K. Sakai, K. Hasumi, A. Endo, Identification of koningic acid (heptelidic acid)-modified site in rabbit muscle glyceraldehyde-3-phosphate dehydrogenase, Biochim. Biophys. Acta Protein Struct. Mol. Enzymol. 1077 (2) (1991) 192–196.
[11] K. Sakai, K. Hasumi, A. Endo, Two glyceraldehyde-3-phosphate dehydrogenase isozymes from the koningic acid (heptelidic acid) producer *Trichoderma koningii*, Eur. J. Biochem. 193 (1) (1990) 195–202.
[12] F.K. Crutcher, A. Parich, R. Schuhmacher, P.K. Mukherjee, S. Zeilinger, C.M. Kenerley, A putative terpene cyclase, vir4, is responsible for the biosynthesis of volatile terpene compounds in the biocontrol fungus *Trichoderma virens*, Fungal Genet. Biol. 56 (2013) 67–77.
[13] M. Mukherjee, B.A. Horwitz, P.D. Sherkhane, R. Hadar, P.K. Mukherjee, A secondary metabolite biosynthesis cluster in *Trichoderma virens*: evidence from analysis of genes under expressed in a mutant defective in morphogenesis and antibiotic production, Curr. Genet. 50 (3) (2006) 193–202.
[14] Y. Shinohara, I. Nishimura, Y. Koyama, Identification of a gene cluster for biosynthesis of the sesquiterpene antibiotic, heptelidic acid, in *Aspergillus oryzae*, Biosc. Biotech. Biochem. 83 (8) (2019) 1506–1513.
[15] S. Pachauri, S. Chatterjee, V. Kumar, P.K. Mukherjee, A dedicated glyceraldehyde-3-phosphate dehydrogenase is involved in the biosynthesis of volatile sesquiterpenes in *Trichoderma virens*—evidence for the role of a fungal GAPDH in secondary metabolism, Curr. Genet. 65 (1) (2019) 243–252.
[16] J. Yang, R. Yan, A. Roy, D. Xu, J. Poisson, Y. Zhang, The I-TASSER Suite: protein structure and function prediction, Nat. Methods 12 (1) (2015) 7.
[17] A. Chaikuad, N. Shafqat, R. Al-Mokhtar, G. Cameron, A.R. Clarke, et al., Structure and kinetic characterization of human sperm-specific glyceraldehyde-3-phosphate dehydrogenase, GAPDS, Biochem. J. 435 (2) (2011) 401–409.
[18] A. Fiser, A. Sali, ModLoop: automated modeling of loops in protein structures, Bioinformatics 19 (18) (2003) 2500–2501.
[19] D. Eisenberg, R. Lüthy, J.U. Bowie, VERIFY3D: assessment of protein models with three-dimensional profiles, Methods in Enzymology, vol. 277, Academic Press, 1997, pp. 396–404.
[20] K. Sakai, K. Hasumi, A. Endo, Inactivation of rabbit muscle glyceraldehyde-3-phosphate dehydrogenase by koningic acid, Biochim. Biophys. Acta Protein Struct. Mol. Enzymol. 952 (1988) 297–303.
[21] K. Zhu, K.W. Borrelli, J.R. Greenwood, T. Day, R. Abel, R.S. Farid, E. Harder, Docking covalent inhibitors: a parameter free approach to pose prediction and scoring, J. Chem. Inf. Model. 54 (7) (2014) 1932–1940.
[22] H. Nakajima, W. Amano, A. Fujita, A. Fukuhara, Y.T. Azuma, et al., The active site cysteine of the proapoptotic protein glyceraldehyde-3-phosphate dehydrogenase is essential in oxidative stress-induced aggregation and cell death, J. Biol. Chem. 282 (36) (2007) 26562–26574.
[23] R.A. Bell, J.C. Smith, K.B. Storey, Purification and properties of glyceraldehyde-3-phosphate dehydrogenase from the skeletal muscle of the hibernating ground squirrel, *Ictidomys tridecemlineatus*, PeerJ 2 (2014) e634.
[24] M.V. Liberti, Z. Dai, S.E. Wardell, J.A. Baccile, X. Liu, et al., A predictive model for selective targeting of the Warburg effect through GAPDH inhibition with a natural product, Cell Metabol. 26 (4) (2017) 648–659.
[25] J.Y. Zhang, F. Zhang, C.Q. Hong, A.E. Giuliano, X.J. Cui, et al., Critical protein GAPDH and its regulatory mechanisms in cancer cells, Canc. Biol. Med. 12 (1) (2015) 10.
[26] S. Ganapathy-Kanniappan, J.F.H. Geschwind, Tumor glycolysis as a target for cancer therapy: progress and prospects, Mol. Canc. 12 (1) (2013) 152.
[27] A.A. Shestov, X. Liu, Z. Ser, A.A. Cluntun, Y.P. Hung, et al., Quantitative determinants of aerobic glycolysis identify flux through the enzyme GAPDH as a limiting step, elife 3 (2014) e03342.
[28] A.V. Snezhkina, G.S. Krasnov, A.V. Lipatova, A.F. Sadritdinova, O.L. Kardymon, M.S. Fedorova, B.Y. Alekseev, The dysregulation of polyamine metabolism in colorectal cancer is associated with overexpression of c-Myc and C/EBPβ rather than enterotoxigenic Bacteroides fragilis infection, Oxidative medicine and cellular longevity (2016) 2353560 2016.
[29] S. Ganapathy-Kanniappan, Evolution of GAPDH as a druggable target of tumor glycolysis? Expert Opin. Ther. Targets 22 (2018) 295–298.
[30] M.A. Robien, J. Bosch, F.S. Buckner, W.C. Van Voorhis, E.A. Worthey, et al., Crystal structure of glyceraldehyde-3-phosphate dehydrogenase from *Plasmodium falciparum* at 2.25 Å resolution reveals intriguing extra electron density in the active site, Proteins Struct. Funct. Bioinformat. 62 (3) (2006) 570–577.
[31] Y.C. Tien, P. Chuankhayan, Y.C. Huang, C.D. Chen, J. Alikhajeh, et al., Crystal structures of rice (*Oryza sativa*) glyceraldehyde-3-phosphate dehydrogenase complexes with NAD and sulfate suggest involvement of Phe37 in NAD binding for catalysis, Plant Mol. Biol. 80 (4–5) (2012) 389–403.
[32] Q. Liu, H. Wang, H. Liu, M. Teng, X. Li, Preliminary crystallographic analysis of glyceraldehyde-3-phosphate dehydrogenase 3 from *Saccharomyces cerevisiae*, Acta Crystallogr. F: Struct. Biol. Crystal. Commun. 68 (8) (2012) 978–980.
[33] M.R. White, M.M. Khan, D. Deredge, C.R. Ross, R. Quintyn, et al., A dimer interface mutation in glyceraldehyde-3-phosphate dehydrogenase regulates its binding to AU-rich RNA, J. Biol. Chem. 290 (3) (2015) 1770–1785.
[34] M. Perucho, J. Salas, M.L. Salas, Identification of the mammalian DNA-binding protein P8 as glyceraldehyde-3-phosphate dehydrogenase, Eur. J. Biochem. 81 (3) (1977) 557–562.
[35] M.R. Hara, N. Agrawal, S.F. Kim, M.B. Cascio, M. Fujimuro, et al., S-nitrosylated GAPDH initiates apoptotic cell death by nuclear translocation following Siah1 binding, Nat. Cell Biol. 7 (7) (2005) 665–674.
[36] N. Harada, R. Yasunaga, Y. Higashimura, R. Yamaji, K. Fujimoto, et al., Glyceraldehyde-3-phosphate dehydrogenase enhances transcriptional activity of androgen receptor in prostate cancer cells, J. Biol. Chem. 282 (31) (2007) 22651–22661.
[37] P.K. Mukherjee, J. Latha, R. Hadar, B.A. Horwitz, TmkA, a mitogen-activated protein kinase of *Trichoderma virens*, is involved in biocontrol properties and repression of conidiation in the dark, Eukaryot. Cell 2 (3) (2003) 446–455.